Mantis: A Scalable, Lightweight and Accessible Architecture to Build Multiform Force Feedback Systems

Gareth Barnaby
Bristol Interaction Group
University of Bristol, UK,
gareth@beam.ltd.uk

Anne Roudaut
Bristol Interaction Group
University of Bristol, UK
roudauta@gmail.com

Figure 1: Mantis is a highly scalable, lightweight and accessible architecture that democratizes haptic devices by allowing to create multiform force feedback systems. E.g. our five implementations: a single desktop-sized arm, a single arm large workspace, a four-arm workspace, a small mobile arm, and a wearable one.

ABSTRACT

Mantis is a highly scalable system architecture that democratizes haptic devices by enabling designers to create accurate, multiform and accessible force feedback systems. Mantis uses brushless DC motors, custom electronic controllers, and an admittance control scheme to achieve stable high-quality haptic rendering. It enables common desktop form factors but also: large workspaces (multiple arm lengths), multiple arm workspaces, and mobile workspaces. It also uses accessible components and costs significantly less than typical high-fidelity force feedback solutions which are often confined to research labs. We present our design and show that Mantis can reproduce the haptic fidelity of common robotic arms. We demonstrate its multiform ability by implementing five systems: a single desktop-sized device, a single large workspace device, a large workspace system with four points of feedback, a mobile system and a wearable one.

Author Keywords

Force Feedback; Robotic Arm; Scalable Architecture; Large Workspace; Multiform; Accessible.

ACM ISBN 978-1-4503-6816-2/19/10…$15.00
https://doi.org/10.1145/3332165.3347909

ACM Classification Keywords

• *Hardware~Haptic devices*

INTRODUCTION

Haptic force feedback devices are a type of haptic system that accurately track position and produce forces. They are particularly used in applications requiring high-precision haptic rendering such as teleoperation, medical training or immersive environments, thus offering users the ability to touch and sense in the digital world. However, current high fidelity devices (e.g. the Phantom 3 [2] or haptic master [28]) are expensive and often confined to research labs whereas more cost effective solutions such as the Phantom Omni [25] are limited in workspace coverage and maximum force.

There is thus a lack of lightweight, easy-to-use, scalable and affordable force feedback approaches. This gap is demonstrated in Haptipedia [13] (a database of haptic devices), in which a number of open-source and affordable solutions are presented, which are all limited in scalability. Kristensen et al. [12] already pointed out this issue and proposed an accessible solution for a hand-sized exoskeleton glove providing locking force feedback. In this paper we fill this gap by tackling the case of 3D force feedback systems that are capable of high power, multiple degrees of freedom and large workspace setups.

We contribute Mantis, an open-source highly scalable and lightweight system architecture that democratizes haptic devices by helping designers to create multiform force feedback systems. It can be used to build accurate, reliable safe and inexpensive systems for use in a variety of scenarios. It allows the creation of not only desktop sized

actuated arms similar in size to the Phantom Premium 1.5 [19], but also large workspace actuated arms to provide feedback in large areas such as CAVE systems [21]. Its modular design enables arrangement of multiple arms for providing multiple points of feedback, and its low weight enables mobile setups such as arms mounted on mobile platforms to provide feedback to lower parts of the body.

The originality of Mantis lies in replacing coreless DC motors and impedance control with low cost brushless DC motors combined with an admittance control scheme. By doing so, it enables the use of significantly lower transmission ratios whilst matching the force capabilities and workspaces of force feedback devices like the Phantom [19]. Mantis also supports direct bi-directional communications interfaces for embedded systems, enabling the use of smart peripheral devices that can be added to the platform to offer more functionality (e.g. Arduinos, Raspberry pi devices).

This paper first outlines the design rationale and system architecture of the Mantis system before demonstrating how it can be used to create multiform systems. We implemented five scenarios: a single desktop sized arm, a single large workspace arm, a large workspace system with 4 arms, a mobile arm and a wearable arm for mobile applications. We enact a series of performance analyses demonstrating the benefits of our system. We show that Mantis can produce devices with haptic fidelity comparable to existing high-fidelity solutions, and that it supports multiple sized workspaces. We also discuss the weight and the costs of our devices in the light of our open-source accessible approach.

We believe our work is of particular interest to the virtual and immersive reality community as well as the Robotic and Haptic communities. Beyond this we think our work could be relevant to the HCI community which has demonstrated an increasing interest in proposing new applications using force feedback systems. Examples include [22][23] which have adapted traditional robots to new interactive scenarios and proposed innovative ways to use force feedback systems. We wish that our work will enable the HCI community to further explore such new direction.

RELATED WORK

We give an overview of force feedback platforms with a focus on accurate and/or affordable solutions.

Force feedback devices overview

We focus on kinesthetic feedback devices which can be classified as locking, one dimension or multiple dimension force feedback. A wide range of existing devices can be found in Haptipedia [13].

Locking devices, such as the wolverine [3] or early versions of Dexmo [12], use small actuators to lock the joints of a mechanical exoskeleton or arm. This restricts the user's movement, creating a perceived force when the user pushes against it. Locking methods have significant power-weight ratio advantages as all the force is created by the mechanical friction rather than an active actuator. This means the devices have small energy requirements making mobility more feasible. However, they lack fidelity as they are an inherently digital on/off (locked/unlocked) system.

1D force devices typically use electric motors to push against the user in one axis. 1D force devices have been implemented within exoskeleton gloves such as later versions of Dexmo [12], VRGluv [29] and CyberGrasp [7]. In the case of exoskeleton gloves, the single axis of feedback is typically aligned to pull a finger towards an open palm pose to simulate gripping an object in the palm or between fingers. Another example is [4] where a 1D force feedback is implemented in a handheld motion controller.

A single axis of feedback allows for simpler and smaller actuators. This allows the feedback to fit into wearable form factors which often means that the feedback provided is ungrounded. This reduces the effectiveness under some circumstances, such as when dealing with anchored virtual objects such as walls or tables, or when manipulating virtual objects with mass. A lack of grounding does, however, mean that wearable 1D force devices can achieve a much larger workspace than grounded devices. Devices such as the CyberForce [6] couple a partial exoskeleton with a grounded arm to provide a point of 3D force feedback around the wrist, and grounding to the exoskeleton. This can improve the realism of the feedback.

3/6D force devices provide force feedback in three or six axes. They can provide highly realistic feedback, although they also require more mechanical parts of higher quality. ForceDimension Omega [10] and the Phantom, typically use coreless DC motors with cable transmissions to achieve high-quality actuators. Other force feedback robots, such as the Haptic Master [28], use control techniques such as admittance control to produce highly accurate force feedback using higher ratio geared transmissions and larger mechanical parts, to achieve larger workspaces. Due to their size and weight, 3D force devices are most commonly implemented as grounded actuators such as the Phantom [19], the Omega [10] and the HapticMaster [28]. Most of these devices are expensive and limited in workspace. This makes many high-fidelity systems inaccessible to many potential users, especially if multiple points of feedback are desired. Industrial robots offer larger workspace but are usually not suitable for sharing workspaces with humans.

One approach to expand the workspace of high fidelity devices is to mount them onto actuated platforms such as in Flying Phantoms [1] where two Phantoms are mounted onto a linear rail. Similar examples include Lhifam [24], HIRO III [8] and [17] where haptic devices are mounted onto the end of larger actuated platforms. These approaches help address the workspace issue but further increase the cost. Other examples of 3/6D force feedback devices include string-based displays such as SPIDAR [15]. These devices can offer good haptic fidelity, and can expand to deliver feedback to multiple points, however, doing so results in dexterity issues caused by the high number of cables required.

Accessible force feedback devices

Despite an abundance of force feedback devices, there is limited work toward providing an affordable and scalable platform for using or building them. Gu et al. propose an accessible, lightweight and inexpensive platform for glove type devices with Dexmo [12]. Their initial design was based on locking force, but they now commercialize a 1D version. However, their system is designed for a hand-mounted exoskeleton and is not scalable to other form factors. There are numerous examples of 3D force devices, such as WoodenHaptics [11], Phantom Omni [25] and Novint Falcon [18], that provide 3D force feedback at a low cost. These devices are limited in the forces they can produce and in scalability - there is little room for adaptation of their mechanical properties. This means current haptic applications must be guided by the pool of available devices. We combine scalability with low cost, meaning Mantis devices can be guided by the needs of applications.

MANTIS REQUIREMENTS AND DESIGN CHOICES

Before explaining how we implemented Mantis it is important to explain the choices we made for the motors, the control scheme and the transmission types. This section starts by laying out our technical requirements and then describes the rationale behind our choices.

Requirements

Our initial requirements echo with our overall approach of creating an open-source scalable system:

- *Scalability*, i.e. allowing arms of multiple length to accommodate for a variety of scenarios.
- *Lightweight*, i.e. being light to be easily clipped onto different locations or be used in a mobile setup.
- *Accuracy*, i.e. offering high-fidelity haptic rendering comparable to existing devices.
- *Accessibility*, i.e. using off-the-shelf materials and fabrication techniques that are relatively inexpensive.

In addition, there is a series of generic technical requirements that are important in any actuated mechanical system:

- *Resolution* refers to the accuracy of the device's position measurement. Similar to pixels on a screen, a *higher resolution* means smaller steps and is desirable for realistic rendering.
- *Torque* (Newton-metres) is a measure of rotational force acting on an object and is proportional to the force produced at the endpoint (where Force = Torque / Distance to pivot). Desktop devices such as the Phantom 1.5 can produce 8.5 Newtons of force.
- *Cogging* is an undesired effect in electrical motors: the magnetic core of a motor attracts the magnets, thus making the motor feel lumpy. An ideal system either uses motors that do not exhibit cogging or compensates for the effect, so the user feels *no cogging.*
- *Inertia* is a force felt when accelerating a mass (when the user accelerates the device). This interferes with haptic rendering and an ideal device would have *no inertia*.
- *Backlash* is an undesired effect in transmission systems where there is a loss of linear transmission due to gaps between mechanical parts (e.g. space or slack between gears). An ideal device has *no backlash*.
- *Backdrive friction* causes users to feel a force when they move the device. As the user moves the device in free space, they are forcing the transmissions and motors to spin, and will feel any friction in these systems opposing their movement. An ideal force feedback device should have *no backdrive friction*.
- *Stiffness* indicates how flexible a device's structure is. As a force is applied to a user, mechanical parts will bend, which will affect the position accuracy of the device. It is usually measured in N/mm (how many Newtons a device can apply before the position accuracy is affected by 1mm) – the spatial rate at which a device can apply force. An ideal haptic device has *a high stiffness*.

Choice of motors (brushless DC)

We use brushless DC motors because they best address the torque and accessibility requirements. We explain our rationale in detail here. There are many types of electric motors and we are particularly interested in the ones for force control rather than position control (e.g. stepper or servo motors). Further, we are interested in motors that produce high torques at low speeds rather than at high speeds such as induction motors. Among force controlled types, the most common are brushed and brushless DC motors. These include subcategories such as coreless DC or slotless motors.

Brushed DC motors [5] are amongst the most common motors and are widely available to buy online in great variety. They are also easy to control by simply adjusting the voltage applied to them. They do, however, suffer from cogging and have relatively low power capabilities. This is due to their efficiency: a typical brushed DC motor is less than 80% efficient, i.e. for a certain amount of energy provided, 80% of it is delivered as kinetic energy, the rest of which is wasted as heat. This energy waste can cause the motor to overheat and hence limits the power consumption and torque output.

Brushed Coreless DC motors are a sub-category of DC motors that reduce cogging. This is why they are widely used in commercial force feedback devices such as the Phantom [19] or CyberForce [6]. They can provide ideal power systems with low back drive friction, no cogging and low inertia. However, they are relatively expensive, and their brushed architecture limits their efficiency as with traditional DC motors. Physically larger motors can be used to provide extra power capabilities, but this comes with increased cost and weight which is not ideal for our requirements.

Brushless DC (BLDC) motors [30] are more complex to control but have a higher power density than brushed motors due to increased efficiency. A typical BLDC motor is around 90% efficient whereas a typical brushed motor is around 80% efficient. The remaining 10% and 20% of energy is converted to heat – a typical brushed motor will produce

around twice as much heat as a typical brushless motor for the same power input. As torque produced is proportional to energy input, a BLDC can, in theory, double the torque of a typical brushed DC for the same energy waste as heat. Recent advances in consumer drone technology have made a wide variety of BLDC motors available at low prices. Most consumer BLDC motors have iron stator cores and so cogging is present although coreless designs (often called slotless motors) exist, they tend to be harder to procure.

Choice of control (admittance)

Admittance control better addresses our requirements of scalability. It compensates for effects such as friction, cogging and inertia and increases accessibility as it allows the use of more readily available BLDC motors, and cheaper, heavier mechanical parts. We explain this further below.

In any haptic system, there is a need to dynamically control the force or position of a mechanical element, typically a manipulator that moves, and where the force position relation is of concern. This is achieved using a control loop, where an electronic system measures some feedback from the device and adjusts an output to control this to a desired value. Force feedback devices most commonly use impedance control and in some cases admittance control, both of which have different advantages and drawbacks.

Impedance control [14] works by measuring the current in the motors for use as an estimate for the real-time force in a control loop. The system senses a displacement and reacts with a force. The nature of impedance control schemes means that mechanical effects are not encompassed within the control loop (the control feedback is taken directly from the motors) and so are not compensated for. This means impedance control schemes require designers to reduce effects such as friction, inertia, or cogging as much as possible. In practice, this means that impedance-controlled devices use high quality coreless DC motors, cable transmissions, high quality bearings and low weight (often CNC machined metal) mechanical parts. These factors lead to high cost of components, manufacture and assembly time. It also means that large workspace devices are impractical due to high inertia from heavier motors and mechanical parts. This is the case for many devices such as the Phantom [19] or Omega [10].

Admittance control [16] is less common and uses force sensors to measure the real-time force exerted on users as feedback in the control loop and reacts with a displacement. The disadvantage of admittance control is that it requires a force sensor, which is not required by impedance-based devices. The nature of admittance control means that any mechanical effects present between the motors and the force sensor (such as friction, inertia or cogging) are encompassed within the control loop and are inherently compensated for. By placing the force sensor at the end of the device, most of these negative effects will be compensated for. This means that admittance control schemes:

- Can adapt to many types of motor and do not need ideal motors as cogging, friction and variations in motor quality are compensated for. This allows systems to use larger and cheaper motors as well as different motor technologies such as BLDCs for increased efficiency.
- Can adapt to many types of transmissions and do not need ideal transmissions (friction and, to a degree, backlash are compensated for). This allows use of cheaper and more practical transmissions such as gears or belts rather than cables.
- Do not require low weight mechanics to reduce inertia (undesired force due to inertia is detected and compensated for). This allows systems to use larger motors and mechanical parts and thus also enables designers to create larger workspace devices.

Choice of transmission types:

Our admittance control scheme allows a great flexibility in transmission type choices. We discuss some easy-to-implement options below. Our prototype devices use direct drive and timing belts.

Timing belt transmission. Timing belts are usually rubber or polyurethane toothed loops. They are commonly used in CNC machines (many desktop 3D printers / laser cutters use them). Many variants of timing belts and pulleys are widely available from various carriers at high qualities and low costs. Some advantages of timing belts are that they are cheap, durable and easy to replace; larger pulleys can be manufactured cheaply with a laser cutter; are fast to assemble; and can be tensioned with an idler pulley to reduce backlash. A disadvantage of timing belt systems is their size. Belts are limited in their transmission ratios most recommendations are for ratios less than 8:1. Multiple timing belt stages can be chained to increase this ratio (e.g. Thrustmaster T300RS wheel [26]), but become less space efficient than other transmissions. Another consideration is their increased friction over cable transmission, but this is not an issue within an admittance control scheme.

Geared transmission. Gears are a common transmission system used in almost every corner of automation. They can produce durable high-quality transmissions in small spaces. Typical gearbox types, such as planetary, are often subject to undesirable effects such as backlash and friction. Friction is of relatively little concern for admittance control solutions, although backlash is still undesirable. Alternative types such as strain wave or cycloidal drives could be used to create simple and compact transmissions with little backlash.

Direct drive (no transmission). A third option is to use no transmission and use the motors in direct drive. This is not practical for most haptic devices due to power limitations of the motors. However, if the system is using high efficiency brushless motors, this can become an option for smaller desktop-sized workspaces. The advantages of this method are simple: no transmission means low cost of parts and assembly, as well as simpler fabrication, although higher power motors are required.

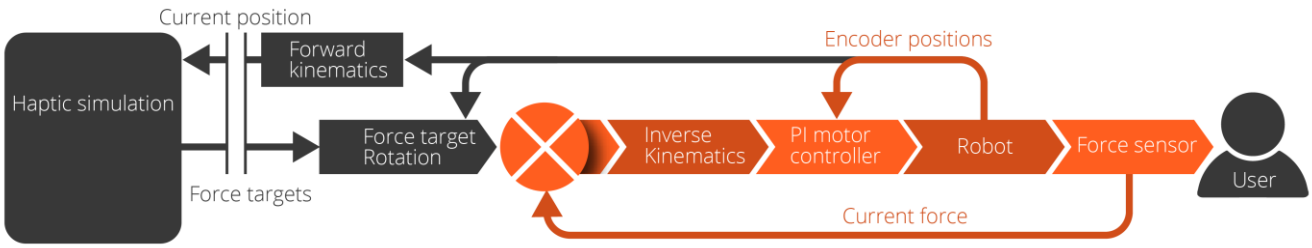

Figure 2: The Mantis control system.

MANTIS IMPLEMENTATION

Figure 3 illustrates the basic Mantis architecture onto which we can adapt an actuated arm of variable length. The system is comprised of a number of key components: a (1) brushless motor controlled through an (2) admittance scheme, driving (3) multiple transmission types. We now describe how we implemented these and provide details for replication.

BLCD motor

We use BLDC motors designed for crop dusting drones (zhxyrc X8308S) measuring 92 * 28 mm, weighing 335g and with a Kv constant of 90 rpm/volt (inversely proportional to the torque constant). They cost 55 GBP. We measured the torque constant of these motors at 0.28 Nm/A (Newton-metres per Amp).

Admittance control

Our control strategy is illustrated in Figure 2 and comprises two control loops. Note that admittance control requires a 3D force sensor and we created our own to keep the Mantis system inexpensive (described in the *Mantis Force Sensor* section). The inner loop is the admittance controller and runs at a rate of 10kHz. The outer loop forms an interface layer to a haptic (physics) simulation and runs at a lower rate of 1kHz. The control system is programmed in C++ with each loop being run in separate hard-timed threads.

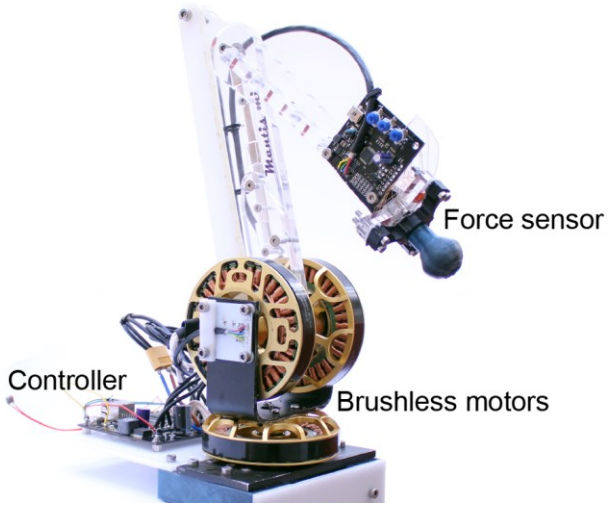

Figure 3: Overview of the Mantis system architecture.

Force target rotation. Force targets in XYZ are given by the haptic simulation. The angles of the force sensor relative to the XYZ space are found from encoder positions. The force targets are rotated in 3D to give targets in XYZ within the coordinate frame of the force sensors.

Inverse kinematics. The current force readings from the force sensors are filtered using a 5-sample rolling average filter (this takes the mean value of the last 5 samples) and subtracted from the rotated force targets to find force errors in XYZ (in the sensors coordinate frame). The errors are put through an inverse kinematic transfer (using positions from the encoders) to find a force error value for each motor.

Proportional–Integral (PI) controller. The errors for each motor are passed into three separate PI (Proportional – Integral) controllers. We found that the PI constants (Kp & Ki) could be dynamically altered to improve system stability and performance over large workspaces – this is useful when using longer arms that have more flexible mechanics.

Robot. The encoders on the robot provide position feedback from each motor in the form of an angle. The force sensor provides measurements of the force between the tip of the robot and the user.

Inverse and Forward Kinematics. The angular position of each motor is used to find the tip position of the device in XYZ. This is sent back to a haptic simulation (usually on a host desktop machine) which checks the device's position relative to virtual objects and returns a target force in XYZ for the device to exert on the user.

Mantis controller

We designed a custom electronic controller unit to control the three BLDC motors that enable three degrees of freedom (3DOF) force devices. A breakdown of the Mantis controller features several elements described below.

- Powerful ARM Cortex M4 microprocessor (MCU)
- Three SPI (Serial Peripheral Interface) bus ports
- Three three-phase digital power amplifier stages (Max 40V @ 20A continuous each – assuming no heatsinking)
- Three ADC (Analog-Digital Converter) channels
- Programmable logic hardware for control signals
- Flexible I/O - Ethernet, USB 2.0 and RS485 connectivity
- 4 x RS-485 Serial Bus channels
- DFU bootloader for easy firmware upgrades via USB
- Low cost (5 for less than 90 GBP of parts per unit)

Microprocessor. We used an ARM Cortex M4 which provides a hardware floating point engine (single precision). This allowed us to perform the rapid calculations required for the kinematics and control systems of haptic robots, as well as convenient I/O capabilities such as SPI, Ethernet, Serial and ADC channels. It also contains onboard flash memory which can store configuration options.

Three separate SPI bus ports [for accurate encoding] allow the microcontroller to communicate with three encoders. We used 14-bit magnetic encoders (AS5047D) that are cheaper than the typical optical encoders used in haptic devices. They also have a significantly higher resolution (16384 counts per revolution – subject to noise of 1 or 2 counts) and provide an absolute angle. These encoders are best utilized as SPI devices, and three SPI ports allow the microcontroller to obtain position updates from three encoders at rates exceeding 20kHz (although we sample at 10kHz).

Three-Phase power amplifiers [for motor control]. BLDC motors are more complex to control than DC motors as the commutation[1] must be performed by the electronic controller instead of by mechanical switches inside the motor. A common technique to control BLDC motors is *sinusoidal drive* which modulates the power in the motor windings according to an offset sine function (a three-phase supply).

Sinusoidal drive is ideal for low speed control. However, it becomes inefficient at higher speeds (due to phase lags caused by inductance in the motor coils). We have assumed that for haptic purposes this is not a problem as we are primarily interested in efficiency at low speeds. However, if using high ratio transmissions, this effect could become problematic. In such a case, sinusoidal control could be adapted by using current measurement combined with Clarke and Park transforms to create a Field Oriented Control (FOC) system that is more efficient at high speeds.

A BLDC motor has three terminals (A, B and C). Each terminal connects to the midpoint of a MOSFET half bridge (or I bridge) on the controller circuit. Each motor requires three half bridges – one for each terminal. A half bridge is made up of two MOSFET transistors, one that connects the motor terminal to V+ (the high side), and one that connects the terminal to 0V (the low side). Each half bridge takes two PWM input signals – one to control the high side and one for the low side. We set the low side to antiphase the high side - when the high side MOSFET is open (letting current flow), the low side MOSFET is closed (stopping current flow) and vice versa. Each half bridge is controlled by a single PWM (Pulse Width Modulation) line from the microcontroller.

All three half bridges (A, B & C) are controlled from the same PWM timer– this ensures all three half bridges are synchronized. If we set each half bridge to a 50% duty, no power is transferred - all the terminals are connected to V+ then, at the same time, are connected to 0V instead (this is why it is important for the PWM signals to be synchronized). If we increase the duty of bridge A (so the high side stays on longer than B & C) we get a current flow from A-B and A-C. As we keep increasing the duty cycle of A, more current flows. To use this to make a motor rotate, first the PWM duty cycles for each bridge are adjusted by a three-phase sine generator function: (where *phase* and *power* are variables):

- ADuty = 50% + sin (*phase*) * *power*
- BDuty = 50% + sin (*phase* + 120) * *power*
- CDuty = 50% + sin (*phase* + 240) * *power*

This produces a holding torque at a point between two magnet poles (north and south) with a strength proportional to *power*. The position between poles is controlled using the *phase* variable (in degrees). If *phase* is continually incremented the motor will turn. To create a torque controller, the motor's current phase position is measured by an encoder, an offset of 120 degrees is added, and used as the *phase* variable of the algorithm above. Given a sufficient program loop speed (We are using 10kHz) the *power* variable will control the torque output of the BLDC motor.

Three ADC channels [for automatic calibration]. Many haptic devices use incremental encoders (e.g. optical) that count steps as they move – they measure a position relative to where they started, although they do not know where they started. The user thus needs to move the device to a known position every time to calibrate it. In some devices, such as [25], this is mediated by a secondary encoder that triggers a (index) pulse in one known position. This requires users to move the device past the index position but makes the calibration easier. To simplify this, we included connectors for three ADC channels that measure potentiometers on the joints of the device. This allows us to measure the starting position without the need for it to be moved past an index point, so a Mantis system can quickly self-calibrate.

Programmable logic hardware [for safety cutouts and power amplifier control]. Controlling our three three-phase amplifiers takes a minimum of 18 PWM signals, where each group of 6 PWM must be synchronized by using the same timer, and of which 3 must be complementary (inverted) signals. This is an excessive number of PWM channels which could not be accommodated by our microcontroller, so we added a CPLD (Complex Programmable Logic Device) to take single PWM signals for each half bridge (9 in total) and generate the high and low side signals. The CPLD also enables ideal safety features, as it can be used to stop the signals to all of the bridges and power down the robot immediately with no reliance on software. We have implemented this feature as a failsafe emergency stop button.

[1] As the motor turns it needs to adjust which coils (electromagnet) have energy flowing in them to make the motor turn. **Commutation** is the process of periodic switching these coils.

Connectivity. Easy connectivity is an important feature, and many robots such as the Phantom premium rely on parallel ports or 1394 firewire interfaces, making them difficult to use with modern desktop machines. Our controller provides options for Ethernet, USB 2.0 and RS485. We included a 100Mbps ethernet interface as all desktop and laptop machines have this on-board. Ethernet also enables the Mantis controller to run a simple web interface.

USB is a highly standardized interface present in almost all desktop or laptop machines. USB is poll-driven, meaning latency is not as low as other methods, although it can easily provide the necessary data throughput - we have successfully tested a stable servo loop with a rate of 5kHz. Data transmission speeds can be limited by physical factors such as cable length. The USB port can also be used to easily upload firmware to the microcontroller via a standard DFU (Device Firmware Upgrade) interface.

We included four RS485 serial ports on our controller. One is dedicated for communications with the force sensor electronics, and three are available for ad-hoc use. These use a differential pair for communications which reduces issues caused by cable length (USB – RS485 adapters are easily sourceable). Each port can provide high data rates (up to 10Mbps) – enough for a 1kHz haptic control loop. The inclusion of the low level RS485 interface also adds a number of unique possibilities:

- One Mantis system can act as a communication hub for multiple Mantis systems to be controlled through a single USB / ethernet link.
- Mantis systems can control or be controlled by other embedded devices such as Arduinos.
- Mantis systems could support peripheral devices (such as foot pedals or external sensors)

Mantis force sensors

An admittance control scheme requires force measurement in three axes. To avoid using onerous three axis load cells, we designed our own three-axis force sensor (Figure 4). It consists of three load cells oriented at 120-degree intervals. Our design is inspired by commercial load cells which consist of 4 strain gauges (a resistive track in a zig-zag pattern on a flexible film) bonded to a material designed to flex in a single direction when force is applied. As the material bends, the gauge flexes and the track resistance changes. The four gauges are wired in a Wheatstone bridge configuration, where the two output lines are fed into a differential amplifier and then to ADC channels on a microcontroller. The force in XYZ can be found by combining the signals from each of the three load cells. We prototyped our sensor in 8mm laser cut Acrylic, bonding 350 ohm strain gauges to it with rapid set epoxy. The end of the force feedback device mounts to the four holes in the middle and a 3D printed end effector section mounts to the six holes around the outside.

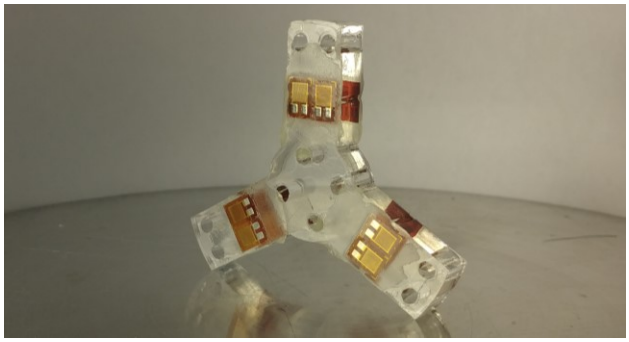

Figure 4: The three-axis force sensor.

We found temperature drift to be an issue with our acrylic prototype. Current flow, user interference, or environmental changes can cause the gauges to heat which significantly effects their resistance. Assuming the temperature change is consistent across the gauges, the Wheatstone bridge will compensate for the resistance change. However, thermal insulation between the gauges (as we have with the acrylic part) results in uneven temperature changes causing sensor drift over time. We mediated this effect through use of 3D printed shrouds to control airflow around the sensors.

Our sensor is configured to read a maximum range of ± 3kg (set using an amplifier gain of 500x). We took a datalog over 1second and measured an RMS signal noise equating to 5 grams. We were unable to detect any hysteresis so we can assume it is less than the noise.

To amplify and read signals from our sensor, we added a circuit to our architecture. This means that the amplifiers and ADC's are placed physically close to the sensors instead of routing the small signals through wires to the main controller (it can introduce noise in large workspace systems). We used instrumentation amplifiers (MCP6N16) as they have a high common mode rejection ratio and should provide good noise immunity when it is impossible to place the sensor electronics near to the force sensors. Each of the three instrumentation amplifiers (one per axis) feeds into a 16-bit differential ADC channel on an ARM cortex M4 and is sampled at 10kHz. The readings are sent via the RS485 interface to the main controller. We found, due to inconsistencies in strain gauge resistance, that it was necessary to add biasing circuitry which was implemented as a potentiometer influencing one output of the Wheatstone bridge via a 25kOhm resistor. This second controller is inexpensive (<30 GBP of parts per unit), and also allows:

- Extension of a Mantis system to 6DOF by using PWM outputs to control three BLDC motors via a secondary power amplifier PCB. There are also 3 ADC ports for position feedback for 6DOF systems.
- A failsafe capacitive sensor in the end effector can be used to pause an admittance control system if the user releases the robot. E.g. if a user lets go of the device, any offsets in the force sensors will cause error windup in the PI controllers causing the robot to lunge unpredictably.

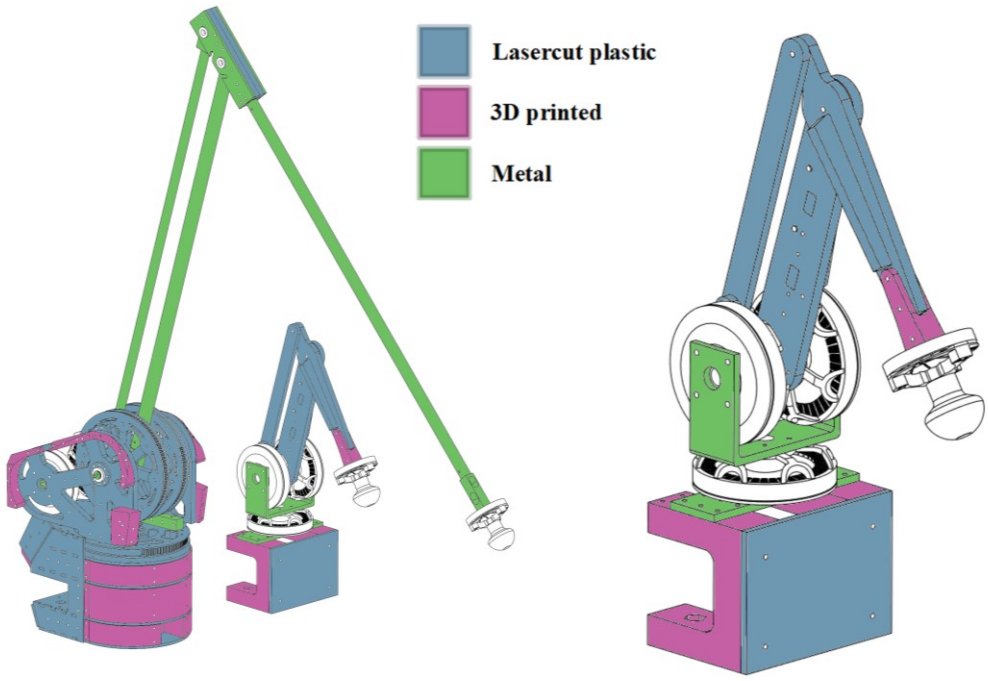

Figure 5. The demonstrator actuator designs for Mantis. Large workspace (left) and desktop workspace (right) Mantis color-coded for fabrication techniques.

MANTIS DEMONSTRATORS

We exemplify the usage of our architecture and demonstrate its scalability in its ability to create multiform systems. We implemented five scenarios illustrated in Figure 1, based around two discrete force feedback devices (desktop-sized and large) built using the Mantis architecture.

Mantis desktop-workspace

We applied the Mantis architecture to a desktop 3DOF force feedback device (Figure 1, Figure 5) with a workspace similar to that of a phantom premium (a reach of 45cm). As illustrated in Figure 5, it uses brushless motors in a direct drive configuration (with a unity ratio parallel linkage for the elbow), along with our force sensor, lasercut 8mm acrylic arm sections, and hand-made aluminum motor mounts. We made a clamp style base designed to fit onto a table from two 3D printed PLA sections and a lasercut panel. The main controller was mounted to another lasercut panel.

Mantis large-workspace

We implemented a large workspace prototype device (Figure 1, Figure 5) with a reach of 145cm which is larger than any device currently commercially available (excluding string based displays), and enough to cover the full reach of a human arm. It uses the same brushless motors with a 7:1 timing belt stage. The structure still largely relies on lasercut parts (acrylic and Delrin) as well as ABS 3D printed parts. The arms are made from aluminum tubing and machined end sections requiring a mill and lathe. We chose to use metal parts as plastic would be more flexible, and breakability could have been an issue with the higher forces present.

Mantis multi-point

We constructed three additional large workspace prototype devices to demonstrate how Mantis can build modular systems. We built a large volume fingertip display (Figure 1) with 4-points of feedback. This delivers 3D force feedback to a finger and thumb on each hand. The design of the base allows the devices to be mounted upside-down (or at other angles) to reduce tangling of the arms when interacting.

Mantis mobile

We further demonstrate how our Mantis systems can create mobile haptic systems by mounting the Mantis-Desktop device on to a wheeled base that was driven by a secondary Mantis controller. The addition of this secondary controller also demonstrates Mantis's ability to interface with peripheral devices, a radio receiver used for wireless control and a gyroscope used for stability control of the base. The secondary controller was linked to the Mantis-Desktop's controller (demonstrating ability as a communications hub), allowing both the movement of the base and the arm to be controlled via the same radio. The platform was powered by a 3-cell lithium polymer battery.

Mantis wearable

We used our large workspace device to demonstrate the low weight of our system and show that it can be used in mobile contexts (Figure 1). We show the device fitted inside a backpack, although it should be more firmly grounded to a user for best operation. Such systems could be particularly interesting for virtual reality applications where larger, mobile workspaces can be desirable.

PERFORMANCE ANALYSIS

We analyze the performance of our desktop and large workspace Mantis devices. We particularly focus on testing the requirements we exposed in the beginning of the paper.

Haptic rendering

Both of our demonstrator devices were tested to stably render smooth spheres with a virtual stiffness of 35N/cm. This comfortably exceeds the minimum threshold for realistic haptic sensation (around 20 N/cm [19]).

Table 1 shows the results of our demonstrator devices with a comparison to several existing commercially available force feedback devices. We found values for the Phantom devices in a datasheet online [20], and for the HapticMaster in [28]. Nominal values are measured with the elbow joint at 90 degrees (~half the device's maximum reach). To gather these metrics for our Mantis demonstrators, we conducted a range of tests that are detailed in this section.

Our tests for maximum force, backdrive friction, and impulse response used a motorized test platform (Figure 6) - a stepper motor that moved a carriage back and forth along a rail. The carriage was coupled to the haptic device via a force sensor (sampled at 10kHz by a Mantis control board). This allowed us to move the haptic devices in a highly repeatable fashion.

Nominal resolution was calculated using trigonometry. The encoder's smallest measurable angle and the distance to the tip at the nominal position are used to find the smallest measurable distance.

Maximum force was found by holding the tip in place and measuring the force output after setting the device to full power (at its nominal position). We also give these results as a torque.

Back drive friction was measured by using the test platform from Figure 6 to slowly move the tip of the test subject back and forth (at 50% of its maximum reach). An average reading was taken from the force sensor in each direction (ignoring impulses from direction changes). This was converted into a friction torque from the tip distance. We did not notice any significant effects due to motor cogging during these tests.

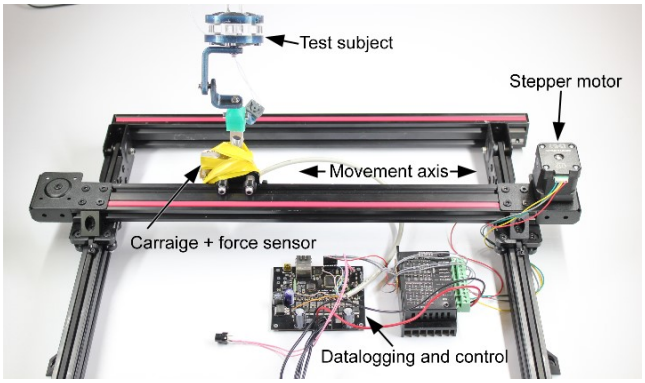

Figure 6: Test platform used for our evaluations.

Nominal stiffness characterizes the flexibility of the mechanical structure (magnitude of displacement caused by bending due to force). This was found by rigidly fastening the test subject's tip in place and observing the change in measured position whilst outputting a force equal to 1kg. We repeated this test for each axis for our demonstrators.

Workspace was difficult to compare because many haptic devices' workspaces are given as an arbitrarily scaled cuboid within the true workspace. We give measurements for an arbitrary sized cuboid, as well as the total useable volume.

Our results show that our desktop-sized and large workspace Mantis devices are comparable to the Phantom series. The only area in which they fell behind was stiffness, particularly the large version. As shown, the stiffness varied significantly between axes (the best axis of the large Mantis matched the Phantom 3.0). This suggests the low values are due to failings in the mechanical design of our demonstrator devices, so it should be possible to achieve significantly better results through further development and testing of these designs.

Inertial Loading

One of our reasons for using an admittance control algorithm was to reduce the inertia perceived by a user. To test for intertia, we used our test platform to rapidly move both of our prototype Mantis devices back and forth rapidly,

Table 1: The haptic characteristics of our Mantis Demonstrator devices compared with Phantoms and the HapticMaster

	Mantis large	Mantis desktop	Phantom 3.0	Phantom 1.5	HapticMaster
Nominal resolution	.04mm (.003 degrees)	.075mm (.02 degrees)	0.02mm	0.03mm	0.008mm
Maximum force	26N (20Nm)	14.5N (3.5Nm)	22N	8.5N	100N
Backdrive friction	32mNM	103mNM	--	--	--
Nominal stiffness (N/mm)	0.25, 1, 0.5 (XYZ)	0.6, 2.5, 2.5 (XYZ)	1	3.5	30
Workspace (cm)	145x120x60 (5100L total)	40x29x20 (116L total)	84x58x41	38x27x19	(80L)

measuring the force impulses upon the rapid direction changes. We also performed the same test on a Phantom premium 1.5 for comparison. A graph of the force impulses from a direction change is shown in Figure 7. All devices were tested with the endpoint at 50% of the maximum reach. Our results show the Phantom premium giving a peak force of around 1150g, and the desktop and large mantis giving 820g and 840g respectively. These results demonstrate the consistency of our admittance control system across multiple form factors, as the much heavier large workspace device produced a similar peak force to the desktop device. It also demonstrates an advantage of admittance control as both Mantis demonstrators produce lower peaks than the impedance-controlled Phantom 1.5.

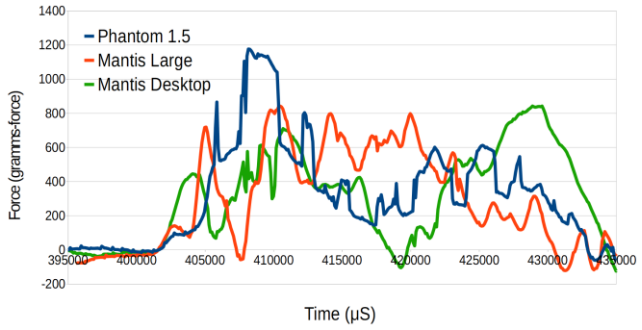

Figure 7: Observed force peak as the device is rapidly accelerated.

Workspace size

We collected some larger workspace examples from the pool of haptic devices existing on the market and compared them with our large workspace device to demonstrate that Mantis systems can achieve considerably larger workspace than existing commercial devices. This is shown in Figure 8.

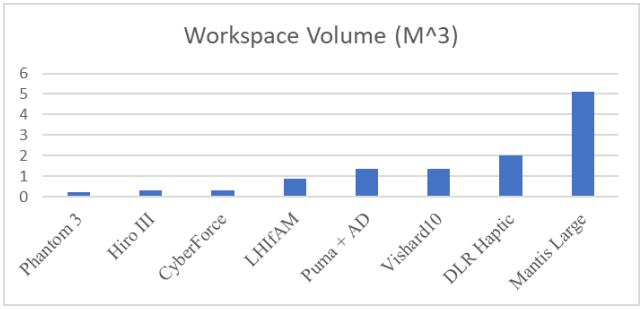

Figure 8: Workspace comparison of large volume devices.

Costs and weight

The combination of direct drive and laser cut parts means that our desktop device costs less than 400 GBP while our large one can be built for less than 600 GBP. Our desktop-sized demonstrator is low in weight (2.3kg) making it ideal for mobile applications although the large one is also still relatively low in weight (6kg) and, as we demonstrated can be worn in a backpack.

DISCUSSION, LIMITATIONS AND FUTURE WORK

We have described the Mantis architecture in detail and demonstrated how it achieves our goals for an accessible architecture for multiform force feedback devices that are comparable in quality to existing high fidelity devices. We found that the mechanical designs of our demonstrators were the bottlenecks when it came to device stiffness, hence we think future work should investigate how to improve stiffness using fabrication materials.

Future work includes investigating the use of further forms of force feedback devices. Here we investigated arm -style designs producing forces suitable for desktop applications; however, the architecture is independent of this form – in theory it can be adapted to any size, shape or force capability. One direction we think is particularly interesting is to investigate applying Mantis to large, high force XYZ cartesian (like many 3D printers) forms with the aim of delivering force feedback to a user's feet, creating a *haptic treadmill* to address current locomotion immersion issues in VR. Another interesting avenue that could be enabled by the direct drive motors we have proven in this context could be miniature 3D force feedback devices for mobile applications such as mobile phones. We would also like to investigate combining Mantis with malleable skin material to create more natural interfaces such as in [27]. Finally, one of our future directions is to use Mantis to create simulation platforms for free-form devices, e.g. augmenting existing ones like [9].

We think force feedback is currently an under-utilized technology within the field of HCI and that it is deserving of greater awareness for creating more innovative interactive scenarios. As argued in our introduction, we think this is due to the accessibility issues surrounding device costs. We have written this paper and implemented this system in the hope that the information we have provided will enable more HCI researchers to access force feedback technology so they can investigate these unique interfaces in their own projects and generate greater exposure and more interesting applications for haptic technologies in general.

ACKNOWLEGMENTS

This work was supported by the Engineering and Physical Sciences Research Council (grant number EPSRC EP/P00s4342/1) and the Leverhulme Trust.

REFERENCES

[1] Barrow, A. L., and William S. Harwin. "High bandwidth, large workspace haptic interaction: Flying phantoms." *2008 Symposium on Haptic Interfaces for Virtual Environment and Teleoperator Systems*. IEEE, 2008.

[2] Chen, Elaine. "Six degree-of-freedom haptic system for desktop virtual prototyping applications." *Proceedings of the First International Workshop on Virtual Reality and Prototyping*. Laval France, 1999.

[3] Choi, I., Hawkes, E. W., Christensen, D. L., Ploch, C. J., & Follmer, S. (2016, October). Wolverine: A wearable haptic interface for grasping in virtual reality. In 2016 IEEE/RSJ International Conference on

Intelligent Robots and Systems (IROS) (pp. 986-993). IEEE.

[4] Choi, I., Ofek, E., Benko, H., Sinclair, M., & Holz, C. (2018, April). Claw: A multifunctional handheld haptic controller for grasping, touching, and triggering in virtual reality. In *Proceedings of the 2018 CHI Conference on Human Factors in Computing Systems* (p. 654). ACM.

[5] Condit, Reston. "Brushed DC Motor Fundamentals." Microchip Technology Inc, http://ww1. microchip. com/downloads/en/AppNotes/00905a. pdf (2004).

[6] CyberForce — CyberGlove Systems LLC [WWW Document], 2019. URL http://www.cyberglovesystems.com/cyberforce/ (accessed 2.19.19).

[7] CyberGrasp – CyberGlove Systems LLC [WWW Document], 2019.URL http://www.cyberglovesystems.com/cybergrasp (accessed 5.4.19)

[8] Endo, T., Kawasaki, H., Mouri, T., Ishigure, Y., Shimomura, H., Matsumura, M. and Koketsu, K., (2010). "Five-fingered haptic interface robot: HIRO III." *IEEE Transactions on Haptics* 4.1 (2011): 14-27.

[9] Flores Cano C, Roudaut A. MorphBenches: using Mixed Reality Experimentation Platforms to Study Dynamic Affordances in Shape-Changing Devices. International Journal of Human - Computer Studies. 12-JUL-2019. DOI: 10.1016/j.ijhcs.2019.07.006

[10] Force Dimension - products - omega.6 - overview [WWW Document], 2019. URL http://www.forcedimension.com/products/omega-6/overview (accessed 2.19.19).

[11] Forsslund, Jonas, Michael Yip, and Eva-Lotta Sallnäs. "Woodenhaptics: A starting kit for crafting force-reflecting spatial haptic devices." *Proceedings of the Ninth International Conference on Tangible, Embedded, and Embodied Interaction*. ACM, 2015.

[12] Gu, X., Zhang, Y., Sun, W., Bian, Y., Zhou, D., & Kristensson, P. O. (2016, May). Dexmo: An inexpensive and lightweight mechanical exoskeleton for motion capture and force feedback in VR. In *Proceedings of the 2016 CHI Conference on Human Factors in Computing Systems* (pp. 1991-1995). ACM.

[13] Hasti S., Fazlollahi, F., Oppermann, M., Sastrillo, J. A., Ip, J., Agrawal, A., & MacLean, K. E. (2019, April) "Haptipedia: Accelerating Haptic Device Discovery to Support Interaction & Engineering Design." Proceedings of the 2019 CHI Conference on Human Factors in Computing Systems. ACM, 2019.

[14] Hogan, Neville. "Impedance control: An approach to manipulation." *1984 American control conference*. IEEE, 1984.

[15] Kim, S., Hasegawa, S., Koike, Y., & Sato, M. (2002). Tension based 7-DOF force feedback device: SPIDAR-G. In *Proceedings IEEE Virtual Reality 2002* (pp. 283-284). IEEE.

[16] LAWRENCE, DALE, and RMICHAEL STOUGHTON. "Position-based impedance control-Achieving stability in practice." *Guidance, Navigation and Control Conference*. 1987.

[17] Luecke, Greg R., and Y-H. Chai. "Haptic interaction using a PUMA560 and the ISU force reflecting exoskeleton system." *Proceedings of International Conference on Robotics and Automation*. Vol. 1. IEEE, 1997.

[18] Martin, S., & Hillier, N. (2009, December). Characterisation of the Novint Falcon haptic device for application as a robot manipulator. In Australasian Conference on Roboticss and Automation (ACRA) (pp. 291-292).

[19] Massie, T. H., & Salisbury, J. K. (1994, November). The phantom haptic interface: A device for probing virtual objects. In Proceedings of the ASME winter annual meeting, symposium on haptic interfaces for virtual environment and teleoperator systems (Vol. 55, No. 1, pp. 295-300).

[20] Phantom premium specifications – 3D systems [WWW Document], 2019.URL https://uk.3dsystems.com/haptics-devices/3d-systems-phantom-premium/specifications (accessed 5.4.19)

[21] Raskar, R. (2000). Immersive planar display using roughly aligned projectors. In *Proceedings IEEE Virtual Reality 2000 (Cat. No. 00CB37048)* (pp. 109-115). IEEE.

[22] Roudaut, A., Rau, A., Sterz, C., Plauth, M., Lopes, P., & Baudisch, P. (2013, April). Gesture output: eyes-free output using a force feedback touch surface. In *Proceedings of the SIGCHI Conference on Human Factors in Computing Systems*(pp. 2547-2556). ACM.

[23] Saraiji, M. H. D., Sasaki, T., Kunze, K., Minamizawa, K., & Inami, M. (2018, October). MetaArmS: Body remapping using feet-controlled artificial arms. In *The 31st Annual ACM Symposium on User Interface Software and Technology* (pp. 65-74). ACM.

[24] Savall, J., Borro, D., Amundarain, A., Martin, J., Gil, J. J., & Matey, L. (2004, April). "Lhifam-large haptic interface for aeronautics maintainability." Proceedings of the IEEE International Conference on Robotics & Automation (audiovisual material). 2004.

[25] Silva A. J., Ramirez, O. A. D., Vega, V. P., & Oliver, J. P. O. (2009, September). "Phantom omni haptic device: Kinematic and manipulability." 2009 Electronics, Robotics and Automotive Mechanics Conference (CERMA). IEEE, 2009.

[26] T300 RS force feedback wheel – Thrustmaster [WWW Document], 2019.URL http://www.thrustmaster.com/products/t300rs (accessed 5.4.19)

[27] Teyssier M., Bailly G., Pelachaud C., Lecolinet E., Conn A., Roudaut A. Skin-On Interfaces: A Bio-Driven Approach for Artificial Skin Design to Cover Interactive Devices. In *The 32st Annual ACM Symposium on User Interface Software and Technology*. ACM.

[28] Van der Linde, R. Q., Lammertse, P., Frederiksen, E., & Ruiter, B. (2002, July). The HapticMaster, a new high-performance haptic interface. In Proc. Eurohaptics

[29] VRgluv - Force Feedback Gloves for VR Training [WWW Document], 2019. URL https://www.vrgluv.com/ (accessed 2.19.19).

[30] Yedamale, P. "Brushless DC (BLDC) motor fundamentals." *Microchip Technology Inc* 20 (2003): 3-15.